

# NANYANG TECHNOLOGICAL UNIVERSITY

---

## SINGAPORE

THE STIMULATING OUTPUT CONFIGURATION OF IMU  
CIRCUIT BOARD AND AN EXPLORATION OF THE EFFECT  
OF PITCHING ON INSECT'S FLIGHT CONTROL.

WU JINBIN

SCHOOL OF MECHANICAL AND AEROSPACE ENGINEERING  
Year 2016/17

**NANYANG TECHNOLOGICAL UNIVERSITY**

**B032**

**THE STIMULATING OUTPUT CONFIGURATION OF IMU  
CIRCUIT BOARD AND AN EXPLORATION OF THE EFFECT  
OF PITCHING ON INSECT'S FLIGHT CONTROL.**

Submitted in Partial Fulfillment of the Requirements  
for the Degree of Bachelor of Mechanical Engineering  
of the Nanyang Technological University

by

**WU JINBIN**

**SUPERVISOR: ASST PROF HIROTAKA SATO**

**SCHOOL OF MECHANICAL AND AEROSPACE ENGINEERING**  
**Year 2016/17**

# Abstract

Insect flight studies have always been of great interests to researchers, which include imitation of insect flight and control of cyborg insects. Being a part of the larger project, Cyborg Beetle Flight Control, this final year project was to develop the IMU circuit board and to explore of the role of pitching during beetle's free flight. For the first half, an IMU circuit board was configured so that it was able to generate four independent channels of analogue output signals that are used to stimulate the flight muscles of beetle. Other configurations regarding to the radio frequency communication were also be done. The second half of the project was to explore the correlations between pitching and flight specifications, like flight height, flight speeds and flight accelerations. Data from free flight experiments were processed and analyzed in MATLAB, which showed correlation between pitch angle and z-speed, and correlation between pitch angle and x-acceleration. The result provides a new systematic method to better control beetle flight, with its speeds and accelerations in a three-dimensional world. Further proof of causality had to be done to provide evidence of causality between these quantities.

**Keywords** Cyborg beetle, IMU circuit board, Pitching, Correlation

# Acknowledgments

The author would like to take this chance to sincerely thank Professor Hirotaka Sato for his thorough guidance and supervision over this project. He has inspired the author to think critically and creatively. The weekly meetings not only helped to keep the author following the schedule but also provided sufficient instructions regarding the experimental direction.

The author would also like to thank Mr Li Yao for his patience and kindness throughout the whole project. Mr Li Yao has been always generously sharing his research experiences and skills with the author. He is a resourceful and talented mentor and friend for both research and life.

And the author would like to thank Dr Vo Doan Tat Thang and Mr Cao Feng for their generous help and instructions on some experimental equipment. And finally, the author would like to thank Mr Chew Hock See for keeping the laboratory equipment.

# Contents

<b>Abstract</b>	<b>i</b>
<b>Acknowledgments</b>	<b>ii</b>
<b>Contents</b>	<b>iv</b>
<b>List of Tables</b>	<b>v</b>
<b>List of Figures</b>	<b>vi</b>
<b>1 Introduction</b>	<b>1</b>
1.1 Background . . . . .	1
1.2 Objective . . . . .	3
1.3 Scope . . . . .	4
<b>2 Literature Review</b>	<b>5</b>
2.1 Biological Background . . . . .	5
2.2 Flight Control . . . . .	6
2.3 Pitch Angle . . . . .	8
<b>3 Implementation</b>	<b>10</b>
3.1 Project Preparations . . . . .	10
3.2 IMU Circuit Board Programming . . . . .	11
3.2.1 PWM Output Fluctuation Range . . . . .	11
3.2.2 Four Channels of PWM Output . . . . .	12
3.2.3 RF Transmission Data Sequence . . . . .	13
3.2.4 Power Management (Power Modes) . . . . .	13
3.3 Exploration of Correlation between Pitch Angle and Flight Specifications . . . . .	15
3.3.1 Experimental Setup . . . . .	15
3.3.2 Data Analysis on MATLAB . . . . .	16

<b>4 Results</b>	<b>20</b>
4.1 Effect of Polyfit . . . . .	20
4.2 Orders of Polynomials . . . . .	21
4.3 Time-shifted Height, Speeds and Accelerations . . . . .	23
4.4 The Effect of Pitch Angle . . . . .	24
4.5 The Effect of Pitch Angular Speed and Pitch Angular Acceleration	28
<b>5 Discussion</b>	<b>30</b>
5.1 Discussion on Data Analysis . . . . .	30
5.2 Recommendations . . . . .	33
<b>6 Conclusion</b>	<b>35</b>
<b>Bibliography</b>	<b>37</b>

# List of Tables

3.1	Effect of timer frequency to PWM output range . . . . .	12
3.2	RF transmission data sequence and units . . . . .	14
3.3	PWM voltage levels . . . . .	14
4.1	Correlation coefficients of Different combinations of polynomial orders . . . . .	22
4.2	Correlation coefficients between pitch angle and other specifications	26
4.3	Average correlation coefficients between pitch angle and accelerations	28
4.4	Correlation of specifications with pitch angular speed and pitch angular acceleration . . . . .	29

# List of Figures

1.1	Cyborg beetle flight control . . . . .	2
2.1	Beetle ( <i>Mecynorrhina torquata</i> ) used in the experiment . . . . .	6
2.2	Horn-worm moth ( <i>Manduca sexta</i> ) in cyborg insect experiment . .	7
2.3	Cyborg beetles created by UCB researchers . . . . .	8
3.1	Motion capture lab . . . . .	16
3.2	Signal amplifier in motion capture lab . . . . .	17
3.3	Cyborg beetle with body coordinate system . . . . .	18
3.4	Comparison between shifted x-acceleration curve and original curve	19
4.1	Comparison between fitted x-speed curve and original data points	21
4.2	Comparison of polynomial fitting among four orders . . . . .	23
4.3	Pitch angle and flight height . . . . .	24
4.4	Pitch angle and flight speeds . . . . .	25
4.5	Correlation coefficients between pitch angle and z-speed with respect to time difference . . . . .	26
4.6	Pitch angle and flight accelerations . . . . .	27
4.7	Correlation coefficients between pitch angle and x-acceleration across different time differences. . . . .	28
5.1	Comparison between curves without prior speeds approximation and that with speeds approximation . . . . .	31

# Chapter 1

## Introduction

### 1.1 Background

For millions of years in evolution, flying insects have developed a unique pattern of flapping flight. The style involving subtle wing kinematics, sophisticated aerodynamics and neural stimulation has confused human for a long history that even today, micro air vehicles (MAV) created by most advanced technology have never come close to what nature has achieved. The MAV created by human has various shortages making it unable to fly as insects do. Lack of sufficient lift from tiny wings, the MAV created was unable to lift its whole weight, which including the most significant weights: motor and battery. Despite having used the lightest material as possible, they are still considered as heavy comparing to insects' membrane wings. In order to have mimicked machine flying in the air like insects and have perfect maneuverability, scientists have kept exploring and conceiving flight mechanism and control strategies by experiences learned from insects. However, because of the diminutive size, the uncertainty and uncontrollable properties of living insects, studies of aerodynamics and wing kinematics were facing great challenges. Therefore, cyborg insect was conceived as a perfect match between pure biological study and engineering implementation. Cyborg insect is made by attaching electrical devices to live insect, creating a robot-insect hybridization. Cyborg insect performs tasks based on stimulation commands, which are a series of electrical pulses generated by the electrical device attached on the insect. Alternatively, there are also other types of implementations for insect control. For instance, chemical was released to disable insects' mobility under control from electrical signals [1]. And another implementation was to create a hybrid system consisting of a large number of complicated bio-microsystems, which were tested with fruit flies (*Drosophila*) [2].

However, restrictions coming from the current technology has limited many facets of cyborg insect research. The relatively heavy electrical devices are still imposing great loads onto the insects. This limits the choice of experimental animals. To be able to carry a circuit board with a battery, the experimental animal has to be large in size and in weight. Only if the proportion of the load to its body weight becomes small, can the insect carry with it without affecting its natural flight gestures. From this point of view, this project used beetles (*Mecynorrhina torquata* of order *Coleoptera*) for experiments due to its relatively large size among insects and its relatively simple and primitive flight patterns. As shown in Figure 1.1, during the experiments, a customized circuit board, assembled with wireless communication unit and IMU sensors, and a battery were mounted onto the beetles. Thus, the choice of relatively large insects for experiments became critical in order to mitigate the effect of weight imposed by the circuit board and battery. And due to the current situation of lacking the essential biological findings, engineering modification on insects remains as a challenging task. For this consideration, beetle is also considered as the best choice for experiment since it possesses a relatively simple flying mechanism and primitive neural control.

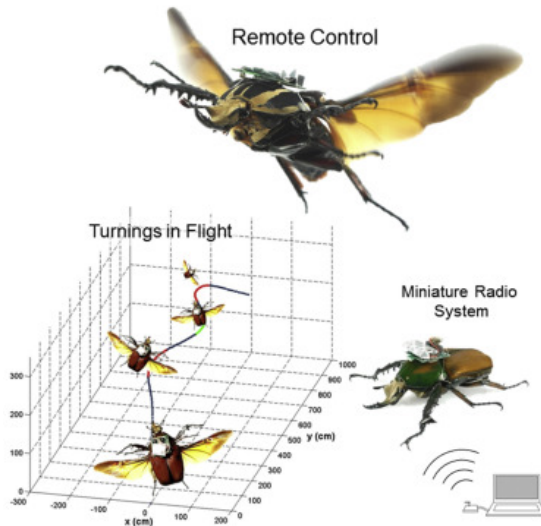


**Figure 1.1:** Cyborg beetle flight control[3]. Experimental setup for remote control of cyborg beetle: the beetle carried with the IMU circuit board which was able to communicate with ground station by radio frequency. The IMU sensor on-board could measure body angles and accelerations, from which flight behavior of the beetle could be calculated and identified. And hence, the effect of using electrical stimulation could be verified as well.

The research of cyborg beetle will deepen human's understanding of the complicated aerodynamics pertinent to flapping wings mechanism, as well as understanding of the biological structure and function of beetle's neural control on muscles. Free control of insect can also be involved in studies of insect communication and social behaviors, as well as studies of foraging behaviors of insects' predators [4]. Cyborg beetle can also be put into use in real battlefield for scouting due to the disguise from its biological appearance and natural flying behaviors. This technique also has bright future for being able to be implemented in civil life for rescuing in disaster where human has difficulty accessing.

## 1.2 Objective

This final year project is a part of a larger cyborg beetle project, which has the aim to create an insect-robot hybrid and grants human ability to control it. For insects, their major mobility is through flight. Hence, flight control is of great importance to beetle control. To control beetle's flight, different flight muscles has to be stimulated by electrical signals, and effectiveness each muscle has over flight control has to be evaluated. Different combinations of muscles will also need to be tested for its possibility of producing better maneuverability control. To investigate these, circuit board with ability to generate multi-channel signals will be favored for this research. The generated signals will need to be independent with each other, with control over specifications setting on each one. Hence, the first objective is to design and program on the circuit board such that it meets the pulse generation requirement. Further improvement on the program will also be done. For instance, power management for standby mode since the capacity of the battery is limited by its size.

To have free flight control, flight height is an inevitable target to be achieve, which will really put flight control over the three-dimensional space. For airplane (fixed-wing flight), pitch angle is crucial during elevation ascending and descending. Inspired by this information, there is also research interest in pitch angle for flapping-wing mechanism. The flight specifications, namely the flight height, flight speeds and flight accelerations, are assumed of close correlation with body attitude. For this situation, pitch angle will be the most evident quantity to be researched on. And hence, here comes the second objective of this project, which is to explore the correlation of pitch angle and other flight quantities (height, speed and acceleration). The other body angles (roll and yaw angles) may also

be investigated for their auxiliary functions in control.

## 1.3 Scope

This report will cover mainly on the correlation investigation. For the first objective of this project, the programming part, clear and brief explanation on design considerations and data representation will be included.

In the literature review chapter, basic biological background of the research animal will be firstly covered, following a review of the past achievements in the field of cyborg insect. At the end, a review of researches pertinent to pitch angle will be given. In the following chapter, implementation, the circuit board programming considerations of the first phase will be illustrated. And then a description of experimental setup for exploring the correlations will be provided. And later the data processing using MATLAB (programming) will be given as well. For the chapter, results from data analysis using MATLAB will be included, which includes three correlations investigations: height, speed and acceleration. Further discussion on validation of correlation and other effects on flight gestures can be found in discussion chapter.

In the following Chapters, the term ‘flight specifications’ indicates flight height, flight speeds and flight accelerations, other than pitch angle. The directions of these flight specifications are according to the body coordinate of beetle body, which is shown in Figure 3.3. However, the direction of VICON data sets obtained from cameras are in accord with the physical dimensions of Motion Capture Lab, which are the direction of length, width and height of the room. The height has a direction of pointing upwards vertically.

# Chapter 2

## Literature Review

The project has been investigated for many years. Before that, scientists tried to build cyborg insect using moths (*Manduca sexta*), while others attempted to investigate flapping-wing kinematics and the underlying aerodynamics using fruit flies (*Drosophila*). The cyborg insect made by hawk-moths were actually attached with a balloon for greater lift due to the relatively small size of the insect. However, for this project, beetles of relatively larger size were used. Thus, load of circuit board and battery is acceptable. The following is a brief review on cyborg insect technology.

### 2.1 Biological Background

The main initiative of this project is stimulating insect muscles by electrical pulses. With proper duration, frequency and voltage, the muscle stimulated will be able to contract accordingly.

The research animal is *Mecynorrhina torquata* (beetle) as shown in Figure 2.1, a subset of *Coleoptera*, which is one of the largest flower beetles in the world. The male adults normally have a body length about 55-85 millimeters, while the female adults have that about 50-60 millimeters[5].

There are two major types of flight muscular control[6]. For some insects like Orthoptera, there is synchronization between neural signals and wing muscle contraction, while for other species like Coleoptera and Diptera, neural signals of lower frequency are observed for faster wing oscillation[7]. For the second type mentioned, instead of directly control wing muscle for each contraction, the neural signals serve as a control signal, which can initiate and terminate the con-

traction state of muscles, and adjust its power and frequency. The simplicity of asynchronous flight muscular control is one of the reason for choosing beetle as research animal. Another reason for the choice is its relatively large size, which grants beetle large carrying capacity of about 3g[2], which in this project is the load from IMU circuit board and battery.



**Figure 2.1:** Beetle (*Mecynorrhina torquata*) used in the experiment. *Mecynorrhina torquata* is one of the largest flower beetles in the world. The male adults normally have a body length about 55-85 millimeters, while the female adults have that about 50-60 millimeters[5]. The animal was chosen as the experimental animal because of their large size, with larger flight loading capacity.

## 2.2 Flight Control

Groups at Cornell University implemented microfluidic devices into moth, shown in Figure 2.2, in which the devices were filled up with a chemical (*neurotransmitter gamma-aminobutyric acid*) that could disable moth's mobility. Injection of the chemical was control by electrical signals, which required a chip to be attached onto the insect. The whole system included a balloon for supporting additional weight of the communication chip[8]. Moreover, implantation of the chip was done before metamorphosis stage of moth, so integration between chip and insect tissue was developed along the metamorphosis process. Since the intruder was placed during the formation of the tissue, the newly developed tissue would heal and produced a robust and reliable tissue-machine interface[2]. The interface allowed the successful control of initiation, cessation and yaw-direction control by a joystick.



**Figure 2.2:** Horn-worm moth (*Manduca sexta*) in cyborg insect experiment[2]. The flight of the moth was controlled by a chemical that can disable the muscle function and deter its mobility. The whole insect-machine system was integrated perfectly since the integration stage was done before metamorphosis of the moth. Hence, the machine and the moth's tissue were well connected and robustly linked.

In University of California, Berkeley, researchers created cyborg insects using beetles, which is the predecessor of this project. Initially, tethered experiments using smaller beetles (*Cotinis*) were carried out, in which beetle optic lobe were stimulated for initiation and cessation control[7]. After that, the larger beetles (*Mecynorrhina*) were involved for free flight experiments of flight initiation and cessation. In both experiment, beetles initiated or ceased by stimulation between brain and posterior pronotum mostly under voltage between 2 and 4 Volts. Further discovery showed that the stimulation on optic lobes (brain) did not affect beetles' steering ability in free flight. Experiments on turning were also done by stimulating on the left and right basalar muscles with positive potential pulse trains (2.0V, 100Hz). Stimulation on left basalar muscle generated a right turn and vice versa. After that, researchers also worked on elevation control by stimulating the optic lobes (brain). Research showed that the experimental beetle (*Mecynorrhina*) would reduce its attack angle (and namely, the pitch angle) by stimulation of 100 Hz on its brain, which resulted an altitude drop of 60 cm for one second of stimulation[9].

Further research will be about how to take advantage of the sensor and energy system on the beetle, namely eyes and energy supply. The vision system will be greatly beneficial to its reconnaissance function, while its energy supply can be used as a battery powering the carried circuit board[2].

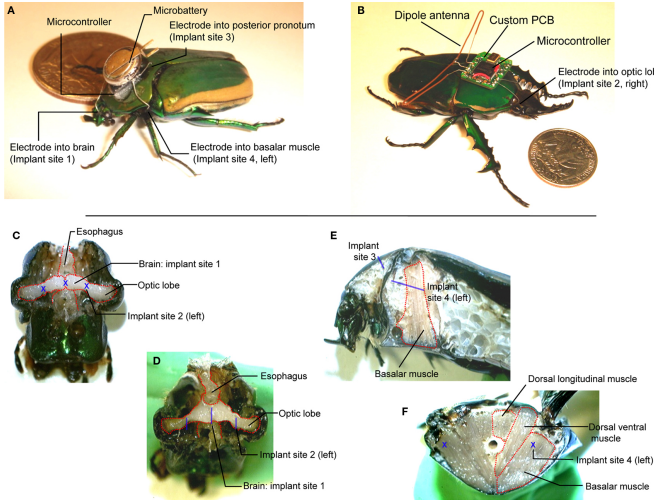


**Figure 2.3:** Cyborg beetles created by UCB researchers[7]. The research group achieved initiation and cessation of beetle flight as well as left-right turning using electrical stimulation. Optic lobes were stimulated under different voltage levels, which initiated or ceased the flight. Optic lobes were also stimulated for elevation control. And basalar muscle was stimulated for left-right turning function.

## 2.3 Pitch Angle

Beetle flight initiation and cessation has been achieved by stimulating optic lobes, while flight turning control has been achieved by stimulating flight muscles (Basalar and 3Ax). For further exploration of flight control, flight height is also an important aspect.

A study using a robotic fly[10] revealed that the equilibrium flight speed of robotic fly during forward flight was greatly affected by the pitch moment, and that fly might switch into different control modes to control pitch moment without changing its lift or thrust production. There was also possibility that the flight speed is affected by a shift in the mean stroke position. The research was done on a robotic fly which emulated a real fly, however, due to the difference in size between them and the relatively simplified structure of the robot, the research could not verify the applicability of the relation on real fly. The research directly inspired the exploration and verification of correlation between pitch angle and flight speed.

Effect of body angles on flight specifications were investigated intensively using fruit fly in the past. A few researches indicated the important significance of pitch angle over flight gesture. During the switch from hovering to small-speed flight, fruit fly tended to shift its center of lift, which generated a pitch-down

moment[11]. From this pitch moment, the stroke plane was tilted to the front, which resulted a forward thrust to drive the body.

And as simulated from 3D model, during the switch from forward flight to hovering flight, fly would theoretically oscillate back and forth due to changing direction of the flapping-wing generated lift[11]. The oscillation pattern was observed such that a pitch-up moment accompanied with a forward translational motion, and then a pitch-down moment accompanied with a backward translational motion. The process repeated giving conditions of friction-free environment and no active control from fly. In the real situation, to avoid this oscillation, fly must perform faster (than the frequency of oscillation) active pitch control to stabilize its hovering position[12]. There are various ways for fly to create pitch moments, but the main underlying principle is to change the relative position of the mean aerodynamics-force center and that of center of gravity[13][14]. Through rotation about pitch axis, counter-torque (flapping counter torque) is generated to stabilize the body.

From the researches illustrated above, it is obvious that pitching moment is an important factor of flight gesture, which can greatly affect flight specifications during forward flight and switch of flight modes. Apart from effects in these mode, pitching moment also functions during saccade, which was performed as a sharp turn and an avoidance pattern of fly[15]. From the study, pitch-down movement was observed during a banked turn, in which the body rotated about yaw axis. The movement resulted in inconsistency of the starting rotation axis and the counter-rotation axis. Studies of the effect of pitching moment will be greatly helpful with the control of cyborg beetle in a three-dimensional space.

# **Chapter 3**

## **Implementation**

This project was divided into a few phases. The first phase was to get familiar with the experimental setup and to studied biological knowledge of the experimental animal. The second phase was configuring experiment apparatuses, mainly the IMU circuit board. And in the third phase, correlations between pitching and flight specifications (height, speeds and accelerations) were being explored and explained.

To verify the effects of pitch angle on beetle flight, flight specification (yaw, roll, pitch and accelerations in three axes) and beetle position (coordination and velocities in three axes) must be recorded by IMU circuit board and VICON system, respectively. By analyzing data obtained in MATLAB, correlations between pitching and flight height, speeds and accelerations can be explored.

### **3.1 Project Preparations**

This project aims to control the flight attitude of the studied beetle by means of stimulating the wing muscles using electric signal. Before achieving controlling beetles, flight specifications had to be obtained from IMU circuit board, which has a 9-axis inertia sensor, and a ground truth system (VICON), which consists of twenty T40s cameras. The collected data was sent from IMU circuit board to a RF transceiver connected to a control computer. Together with the data collected from VICON System, data were written into files for later processing. Besides collecting data, the IMU circuit board is also able to generate electrical signals to stimulate wing muscles. The voltage of electrical signal is generated and controlled using Pulse Width Modulation (PWM).

Meanwhile, study of the experimental animal was also conducted. Anatomy of beetles and wiring connecting between beetles and IMU circuit board were practiced several times. From anatomy, several muscles were identified, located and studied: dorsal longitudinal muscle, dorsal ventral muscle, basalar muscle, subalar muscle and the third auxiliary muscle (3Ax). For flight turning control, basalar muscle and the 3Ax muscle have significant control function, while the subalar muscle possesses limited effect. Beetles perform responding turning when the ipsilateral 3Ax muscle or the contralateral basalar muscle being stimulated. Implantation of stimulation wires into experimental beetles was also practiced. After holes on beetles' cuticles above the investigated muscles being made by insect pin, electrodes were implanted into investigated muscles through holes, with one pair of positive and negative electrodes on one muscle. Electrodes are made of silver wires coated by Teflon, whose one end were soldered onto IMU backpack. The other end of the silver wires was flamed to remove insulating barrier before being implanted into beetles' muscles. Beeswax was then melted and applied onto the opening of holes to ensure the wires were tight and immobile.

The VICON system uses infrared light for object detection, which required the detected objects to bear a reflective tape. Hence, the battery is wrapped by reflective tape to enable detection by VICON's cameras, and then it was attached above the circuit board.

## 3.2 IMU Circuit Board Programming

### 3.2.1 PWM Output Fluctuation Range

At the early stage of the circuit board program, PWM output was tested by oscilloscope, but undesired characteristic was observed. The output signal range varied with timer frequency that was set by the microprocessor on IMU circuit board. A small experiment was carried out to investigate the relationship between timer frequency and output range, and the result is shown in Table 3.1. The decreasing value in second column is because of the usage of power in battery. Channel 1 was set as 255/256 of full voltage of the full battery capacity, while channel 2 was set as 156/256 of full battery. The fourth column was the changing range of channel 2 voltage. The theoretical channel 2 voltage was calculated using channel 1 voltage. From fourth column, tendency is clear that higher timer frequency has narrower range of output voltage. The center points of channel 2 voltage ranges were corresponding to the theoretical channel 2 voltage, which

indicated that channel 2 voltage was fluctuating around the center value, and that the range is decreasing as increase of timer frequency. Thus, higher frequency generates a more accurate output.

**Table 3.1:** Effect of timer frequency to PWM output range. The fourth column is the fluctuating range of voltage output by channel 2. The range narrows down as the frequency of timer increases. Channel 1 represents the nearly full capacity of battery, serving as a comparison for channel 2 and for calculation of theoretical voltage.

Frequency of Timers (Hz)	Channel 1 Voltage (V)	Channel 2 Voltage Range (V)	$\Delta$ of Channel 2 (V)	Theoretical Channel 2 Voltage (V)
4M	3.92	0.40 - 3.84	3.44	2.40
8M	3.84	1.12 - 3.44	2.32	2.35
16M	3.84	1.60 - 3.12	1.52	2.35
32M	3.76	1.80 - 2.52	0.72	2.30

To achieve a more accurate output voltage, either increasing the timer frequency or changing the oscillator on the circuit board can be done. However, timer frequency has its built-in limit, which is 32MHz for the microprocessor used in this experiment. Experiment required range less than 0.2V to have precise voltage control. To change time constant of the oscillator, either resistors or capacitors must be increased. The resistors were later found to be unable to increase since it would become a voltage divider and affect the actual voltage of beetle muscle. Therefore, capacitors in the oscillator was augmented to eight times of the originals. After this calibration, IMU backpack is now able to produce a relatively accurate PWM output.

### 3.2.2 Four Channels of PWM Output

The IMU circuit board was planned to be able to generate four independent channels of PWM output for controlling four pieces of different muscles. Each pair of two channels are controlled by one timer. Channel 1 and 3 are controlled by Timer 3 (T3C0 and T3C1, respectively); while channel 2 and 4 are controlled by timer 4 (T4C0 and T4C1, respectively). Each channel is able to independently output electrical pulses, which have certain duration, frequency, peak time, voltage and latency set by user. Voltage is controlled using PWM since the circuit board can only output two voltage levels, which are zero and the voltage value of the battery. Single channel can generate output alone without interference from other others, and two different channels can generate PWM output simultane-

ously without affecting each other. With this feature, multiple muscles can be studied at the same time, as well as the synergy of different muscles.

Since different muscles are interconnected inside beetle, it is necessary to set the idle channels as high impedance to remain uninfluenced from the working channels. The microprocessor used has function to set output pins controlled by timer 3 as three-state (high impedance) mode. However, pins controlled by timer 4 do not possess similar function. Hence, to avoid interference, these pins controlled by timer 4 were set as input mode in idle state. When two channels controlled by timer 3 pulse at the same time, setting three-state mode is infeasible for that high frequency. Hence, in this situation, the two channels are assumed to have limited effect on each other.

### 3.2.3 RF Transmission Data Sequence

The command of electrical pulse output is generated by the computer terminal, which is a sequence of data representing the intended controlling channel(s), duration(s), frequencies and other specifications. For RF transmission, delay time during transmission is always undesired. The data sequence is designed as such that fewer bytes are used to deliver full information. As shown in Table 3.2, different bytes represent different specifications of different units, as listed in the third column. From byte No.2 to No.5 represent specifications of the first channel, while from byte No.6 to No.9 represent that of the second channel. The last byte represents starting latency of channel 2 relative to channel 1, assuming that channel 1 is always leading channel 2 since during the experiment, different channels can be easily changed by swapping wires.

The PWM voltage in Table 3.2 has values from 0 to 15, which is due to quantization of the continuous voltage range. The full voltage value of battery is divided into 16 ladders, from 0 to 15, each represents a corresponding voltage level. Table 3.3 showed the corresponding duty cycle of different voltage levels. Level 0 has the highest voltage while level 15 has the lowest.

### 3.2.4 Power Management (Power Modes)

The IMU circuit board was programmed with two power modes to improve efficiency of battery usage and lengthen its working time. One is working mode, and

**Table 3.2:** RF transmission data sequence and units. The transmitted data sequence, except for the first and last byte, is divided into two parts, representing the controlling parameters of the two channels. The first byte indicates the timer number to be started, while the last byte indicates the signal delay between these two channels. Channel that is not used will be set as zero for output duration byte.

Byte Number	Representation meanings	Units
1	Timer number: 3 or 4	–
2	Duration of first channel	50 microseconds
3	Frequency of first channel	5 Hz
4	Peak-time Period of first channel	1 microsecond
5	PWM voltage of first channel: 0 - 15	–
6	Duration of second channel	50 microseconds
7	Frequency of first channel	5 Hz
8	Peak-time Period of first channel	1 microsecond
9	PWM voltage of first channel: 0 - 15	–
10	Latency between two channels	10 microseconds

**Table 3.3:** PWM voltage levels. The voltage levels represent the percentage of the full voltage output, with zero indicating the highest voltage level and 15 indicating the lowest.

voltage level	PWM duty cycle
0	240/256
1	224/256
2	208/256
3	192/256
4	176/256
5	160/256
6	144/256
7	128/256
8	112/256
9	96/256
10	80/256
11	64/256
12	48/256
13	32/256
14	16/256
15	0/256

the other is idle mode. In the idle mode, the circuit board does not transmit the IMU sensor data to the computer terminal. The initial intention was to switch off the 32MHz oscillator and leave the 16kHz oscillator for other functions. However, this was not possible since once the 32MHz oscillator was turned off, the radio frequency unit would be turned off as well, which would prevent the circuit board from receiving data from the computer terminal. And hence, the circuit

board would not be turned on again once it was turned off. The reason to set an idle mode is to prevent power waste when the circuit board is calibrated at the beginning of every turn-on or when the tested beetles fall to the ground, which ends a test. The circuit board is programmed as such that switching between different power modes executes when it receives different data strings ('AWAKE' or 'SLEEP') from computer terminal. The initial state of the circuit board was set as idle mode to prevent battery use in the early stage, so the experiment would start after sending activation signal to activate the data transmission process.

### **3.3 Exploration of Correlation between Pitch Angle and Flight Specifications**

Experiments were done in the motion capture lab to explore the correlation between pitch angle and height, speeds and accelerations. After that, MATLAB data analysis was performed to extract the correlations from obtained data.

#### **3.3.1 Experimental Setup**

To obtain natural flight response from beetle, the experiments were performed within a large empty room with motion capture system. Motion capture lab was installed with a VICON motion capture system which consists of 20 infrared cameras. The focus zone of this camera system has a length of about 9 meters, widths about 6 meters (not strictly rectangular). The walls are covered with white-color paper sheet to form a uniform environment and to reduce unwanted distraction to the beetles during the experiments (Figure 3.1).

After switching on the VICON hardware, a RF transmitter, which was connected to the computer, was connected to the signal amplifier (Figure 3.2). Software Nexus provided by VICON company was started and configured for a new test. A LABVIEW program running on computer side was also started for collecting data and issuing commands to the circuit board. To start the test, the beetle was released at the edge of detection area. The beetle was in free fly mode while carrying the circuit board and a reflective-surface battery. These two devices were adhered to the pronotum of the beetle by tape. IMU sensor measuring the body angle and acceleration transmitted data to the ground station while the ground station issues stimulation instruction back to the circuit board.



**Figure 3.1:** Motion capture lab. The room is covered with white color paper with 20 infrared cameras on the top, which belong to the motion capture system. The focus zone of the capture system has a range of about 9 meters in length and 6 meters in width.

### 3.3.2 Data Analysis on MATLAB

The structure of raw data collected during experiments consists of data from VICON, sensor and control signal record. Since the system was designed for both sensing and controlling, the control signal record was remained in the raw data. For this project, the control signal record was not used and the records had to be removed in later processing. The VICON data streams are in the format of four sets. The first set is the record time since the beginning of recording. The following three sets are x, y and z coordinates, respectively. The sensor data streams are in the format of seven sets, which are record time, yaw angle, roll angle, pitch angle, x-acceleration, y-acceleration and z-acceleration, respectively. The accelerations obtained in IMU sensors were not accurate enough for computing velocity and position, and that is why VICON was used for positioning.

The raw data obtained from VICON system and sensor were imported and stored as two matrices: viconData and sensorData. There were ‘gaps’ in viconData since during the experiments beetles often flew out of the detection area. Hence, the viconData was then segmented into several parts which have continuous data output. Segments that had less than 15 sets of data were discarded due to their insufficiency of information and unpredictable manner within the data gaps. And then the x-direction, y-direction and z-direction speeds were calculated for each viconData segments by taking derivatives of position points and then taking the average of two adjacent derivatives. Horizontal speed was obtained by combining x-direction and y-direction speeds. Apart from that, the motion direction of the flying beetle was calculated by taking the inverse tangent of the ratio of y-direction



**Figure 3.2:** Signal amplifier in motion capture lab. The beetle was controlled remotely by radio frequency. Due to the insufficient transmission power of the micro-controller, amplifier had to be used for long-distance communication.

speed over x-direction speed. Accelerations were then calculated similarly from the speeds obtained from the above steps. The obtained three components of accelerations are actually following the ground coordinate system with fixed x, y, and z directions. However, in this project, one of the goal is to explore the correlation between pitch angle and accelerations. Only when the accelerations were aligned with the motion directions can this correlation be explored and studied, since the rotation of the pitch angle (pitch axis) was perpendicular to the motion direction of the flight. Hence, the three calculated components of accelerations were then transformed into the body coordinate of the beetle, namely, with x direction along the longitudinal direction of the beetle body, y direction within the same horizontal plane as x direction and z direction unchanged, as shown in Figure 3.3.

The sensorData was filtered to remove large changes and unexpected extremities in pitch angle, since those were generated by system noises and would affect the following calculations and analysis. Then the sensorData was also segmented for the same period as that of viconData, since sensorData was more stable and there were many parts in the raw data where only sensorData were received by the laptop terminal. Hence, the segmentation was based on viconData. For each segment of sensorData, a polynomial of certain order was fitted into the pitch angle data. This step smoothed pitch data and countered some fluctuations. After

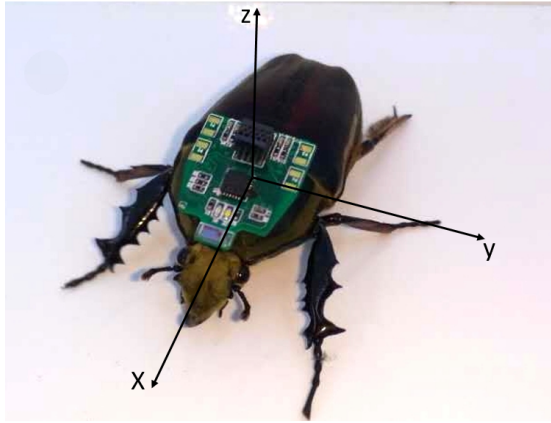


**Figure 3.3:** Cyborg beetle with body coordinate system. The local coordinate system has an origin at the centroid of the circuit board since the IMU sensor is located on it. Y axis is pointing horizontally to the left of the body, which resulted in a positive pitch angle when the beetle pitches down.

fitting the curves into data segments, new values of pitch angle would later be calculated based on the new polynomial curves for every instant.

To compare and obtain correlation between pitch angle and height, speed and acceleration. The three quantities, height, speed and acceleration, had to have the same time instant as the pitch angle, which means at one instant, there were both pitch angle data, height data, speed data and acceleration data. And the height of flight is the z position from VICON data. To achieve that, these flight specifications (height, speed and acceleration) were fitted with polynomials of certain order to have approximation in some instants where these quantities did not exist. Then from these fitted polynomials, new values of the three quantities at same instants with the pitch angle data were calculated. Before the calculation, the time variable was shifted with a steps of 0.02 second (illustrated in the following paragraph). The newly calculated data would be used for exploration of correlation between pitch angle and the three quantities.

To explore correlation between pitch angle and those three quantities, correlation coefficients between each pairs of quantities were calculated. There is a built-in function in MATLAB for calculation of Pearson's correlation coefficients, which returns a matrix of coefficients between different columns. For the calculation of correlation coefficients, there was one more consideration. The time difference between pitch angle and the other quantity was not known and needed to be explored. That means a change in pitch angle will not immediately impose a change in the other quantities. There is certainly a response time between these

two quantities. To verify that, pitch angle data was remained unchanged while the other quantities (height, speed and acceleration) were shifted along the time axis at a fixed small step to find the maximum value of correlation coefficient. Figure 3.4 showed the comparison between the shifted x-acceleration curve and the original curve at a time difference of 0.2 second (red curve was shifted towards the positive direction of time axis, which produced the green curve). In the MATLAB programming process, a step of 0.02 second was set for the shift of quantities. The total duration of the shift depended on different quantities since some quantities might have a longer response time, which required a longer time shift for the best fit. In the end, tables consisting of time difference and correlation coefficients was obtained and exported as excel files. Further analysis on these generated table was done on Microsoft Excel and Jupyter Notebook.

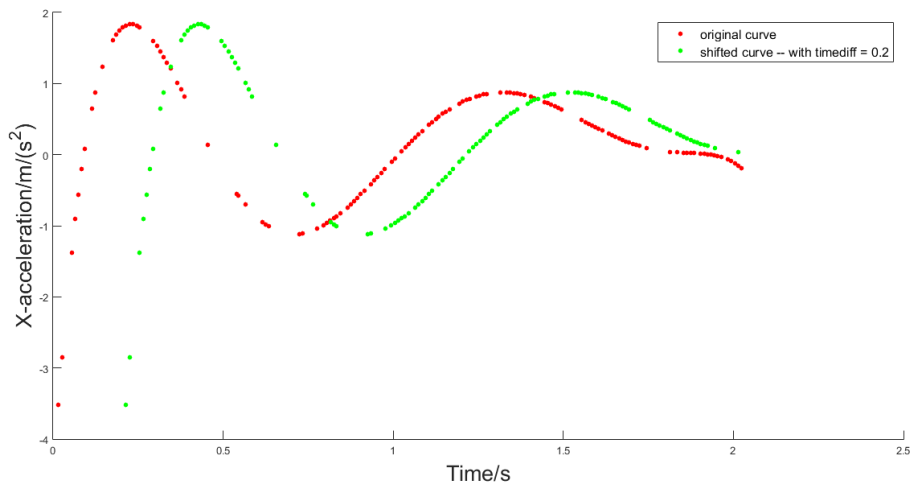


**Figure 3.4:** Comparison between shifted x-acceleration curve and original curve. Different quantities had different response times. Thus, to find out the maximum correlation coefficients between two quantities. One of the quantities (in this case, x-acceleration, was shifted along the x axis before the calculation of correlation coefficients.

On Microsoft Excel, correlation coefficients of same time instant and same quantity were grouped together and averaged, and then graphs were plotted based on the averaged coefficients.

# Chapter 4

## Results

There are 15 beetles involved in the studies, with each beetle being tested for an average of 5 times (Since some of the data sets are too short to be used for calculation). Firstly, curves of flight specifications and pitch angle were plotted for a view of the possible underlying rules. Then the correlation coefficients were calculated for different pairs of pitch angle and flight specifications. For the calculation, consideration of response time was also considered and manipulated for the best fit. Abnormal behaviors were also analyzed to have better understanding of beetle flight behavior.

### 4.1 Effect of Polyfit

As illustrated in the last chapter, polynomials were used to smooth and fit the collected data points. The purpose was to fill up all the gaps between the discrete data points, to prepare for the next operation of synchronizing the time stamps with those of pitch angle. Figure 4.1 showed a comparison of the fitted x-speed curve and the original data points. The green curve represents the order-6 polynomial which was fitted to the original data points, which are represented by the black color markers. From the figure, it can be observed that the polynomial curve fitted the original data points well and reduced the noises and drastic fluctuation resulted from system constraints and unexpected error. The fitted curves convey clearer views of the characteristics of data, and helped to identify the interested underlying patterns. Approximation of pitch angle, height, speeds and accelerations were also performed.

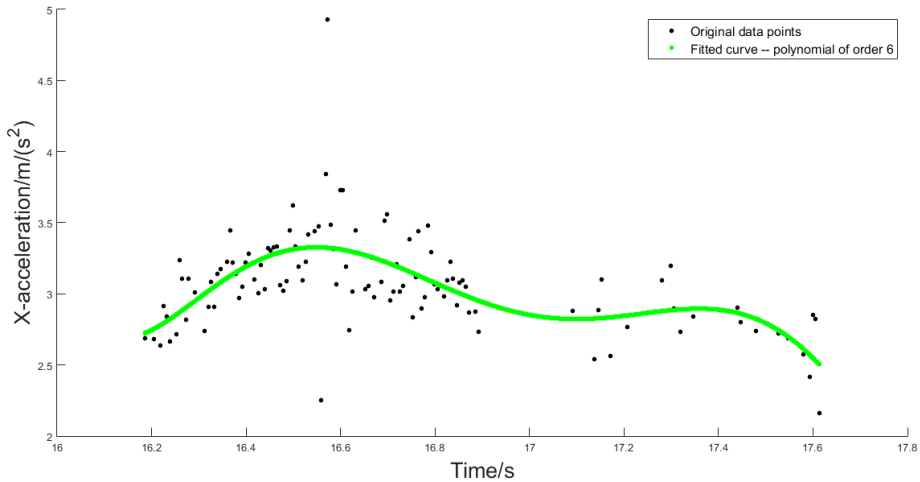


**Figure 4.1:** Comparison between fitted x-speed curve and original data points. Polynomials were used to approximate the original data. In this plot, black dots are the original data points while the green curve is the approximated polynomial. The approximation reduces the effect from some extreme values and provided an estimation on instants when there were no data.

## 4.2 Orders of Polynomials

To smooth the collected data and predict the values at blank sections in the data stream, curves were fitted into the original data points. The original data were segmented into pieces, which contain small numbers of continuing data points. Due to the frequent occurrence of gaps and the purpose of utilizing as much data as possible, the threshold of segmentation was set as 0.5s. That means pieces with gaps shorter than 0.5s were not segmented into shorter pieces, and the gaps were approximated by the polynomial curves. Approximating the data points using a curve and comparing correlation between different curves require a certain length of data points. It cannot be too short, otherwise the generated curve is not representative enough. Hence, the segmented pieces were inspected and filtered with minimum length of 2s. The segmented pieces are relatively short, so polynomials instead of splines were used for curve fitting.

In the program, the accelerations of beetle flight were calculated by taking the derivatives of speeds. However, since the speeds were calculated from VICON position data, the fluctuation was quite huge along time. Smoothing the data using polynomial curves will certainly reduce the fluctuations and errors, but the processed data might lose the genuine information contained in the original data. Hence, in order to decide whether to approximate the speeds data before

calculating accelerations. A comparison was done. The comparison set different orders of polynomials that approximated pitch angle and the accelerations data (The acceleration data was approximated after being calculated in order to obtain the correct time stamps as those of pitch angle). And then the correlation coefficients of the obtained time series were calculated and averaged. In the end, the averaged correlation coefficient of not approximating the speeds data before calculating accelerations is 0.409, while that of approximating speeds before calculating accelerations is 0.752. The result shows clearly that the original speeds had to be approximated before calculating the accelerations. Further explanation will be provided in the Discussion session.

**Table 4.1:** Correlation coefficients of Different combinations of polynomial orders. The first row represents the order of the polynomial that is used to approximate x-acceleration, while the first column represents that of the pitch angle.

pitch/Acc	4	5	6	8	10	12
4	0.697	0.706	0.686	0.679	0.680	0.676
5	0.714	0.767	0.751	0.748	0.747	0.743
6	0.725	0.780	0.763	0.761	0.759	0.755
8	0.705	0.770	0.759	0.762	0.758	0.755
10	0.691	0.757	0.745	0.754	0.750	0.748
12	0.682	0.747	0.735	0.742	0.741	0.738

Table 4.1 shows the correlation coefficients of different combinations of polynomial orders, with the first row depicting the order of polynomial approximating x-acceleration and first column depicting the order of polynomial approximating the pitching angle. As it is shown in the table, the maximum correlation coefficients between pitch angle and x-acceleration occurs when the order for pitch angle is 6 and that for x-acceleration is 5, which is 0.780. However, the deviation of the values is not that large.

As shown in Figure 4.2, different orders of polynomials were tested to approximate the original data points. Polynomials of lower orders tend to lose more significant information of the original data points, but they reduce noises and undesired errors and are impervious to extreme values. In contrast, higher order polynomials are better fitted into data, but there are higher chances of over-fitting. Normally, the order of fitting polynomial should not be larger than half of the number of data points. As it is observed from Figure 4.2, order 10 was chosen to fit the

pitch angle, since it fitted the data points well and had relatively little vulnerability to extreme values. Polynomials of order 15 and 18 fitted the original data better, however, they require more computational power and increase the chance of over-fitting. Although Table 4.1 shows the maximum value occurs when the orders of polynomials takes low values, the curves generated might not fit the original data well. Hence, the final decision for orders of polynomials for pitch angle and x-acceleration are 10 and 5, respectively.

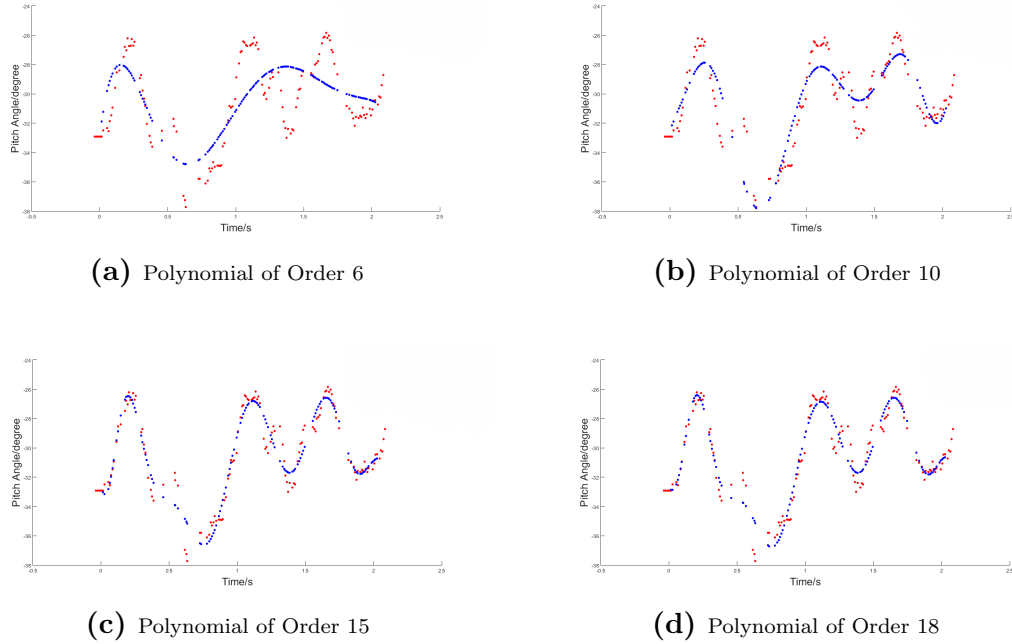


**Figure 4.2:** Comparison of polynomial fitting among four orders. The blue curves are the fitted polynomials and the red dots are the original data points. Different orders of polynomials were fitted into the original pitch data set to find out the best approximation. The higher order a polynomial has, the best can it fit into the data, but greater chance of over-fitting it possesses. Higher order approximation also requires more computational power.

### 4.3 Time-shifted Height, Speeds and Accelerations

Flight specifications were shifted and corrected to the same time stamps as the pitch angle allowing a computation of correlation coefficient between them. For this process, after performing curve fitting, the corrected values were then calculated from the resulted polynomials by setting the time stamps same as the pitch angle. The time series used for obtaining values of flight specifications from polynomial curves were taken from pitch angle data sets. The parts of data from

both pitch angle and flight specifications that were not overlapping, were deleted. As shown in Figure 3.4, the corrected results contain the essential information in original data and act as reasonable and proper approximation of the original data.

## 4.4 The Effect of Pitch Angle

In figure 4.3, one of the flight trial exploring the correlation between pitch angle and flight height was displayed with respect to time axis. The vertical axis represents the magnitude of the two quantities. The left axis in degree, and the right one is in meters. The blue color line is the pitch angle, while the brown color line is the flight height. The pitch angle data (sensor) is more consistent as compared to the discrete-segment pattern of the height data (VICON data) during the collection process, which is due to the physical constraints of the camera area. The experimental beetles were easily fly out of the effective region, which resulted in a blank in data sets. Hence, in order to compare these two quantities, the pitch angle data was cut short as the height data for the same time periods. From the plot, correlation between these two quantities cannot be clearly observed.

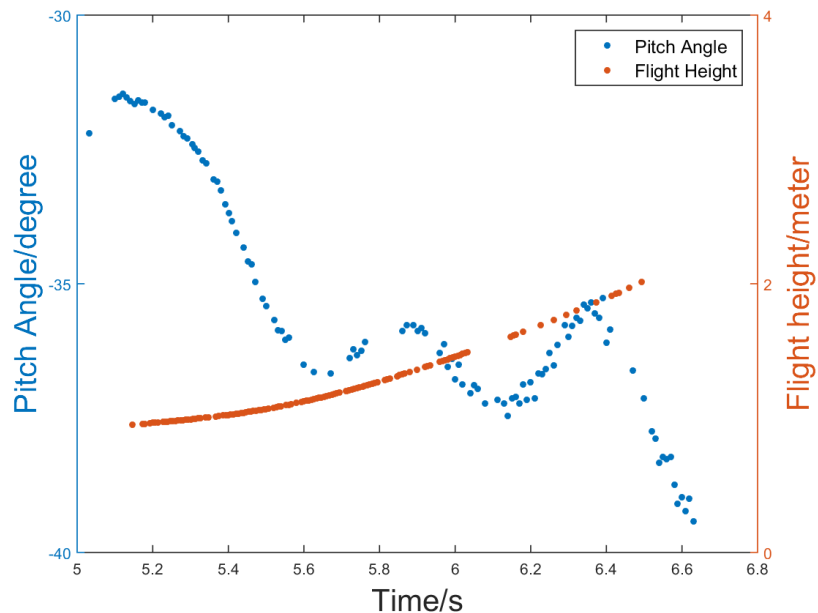


**Figure 4.3:** Pitch angle and flight height. The x axis represents time while the two y axes are pitch angle and flight height, respectively. The blue color line represents the pitch angle and the brown color line represents the flight height. From the plot, little correlation can be observed.

After exploring the correlation between pitch angle and height, that between pitch angle and speeds was also done. The changes of pitch angle and speeds along time axis are shown in Figure 4.4. The brown, yellow, purple and green lines represent speeds in x, y, z and horizontal directions, respectively. The horizontal speed is a combination of x and y speeds. Intuitively, from the plot, the purple line (time-corrected z direction speed) and the blue line (pitch angle) appear to have negative correlation. The observed result matches the initial conjecture. The negative values is from the direction settings of the pitch angle and vertical speed. When a beetle pitches down, the pitch angle increases and it was proposed that the speed will also increase. However, the heading direction of the beetle is pointing downwards, which results in a speed increase in the negative axis (The direction of the vertical speed points upwards), and that was seen as a decrease of vertical speed.

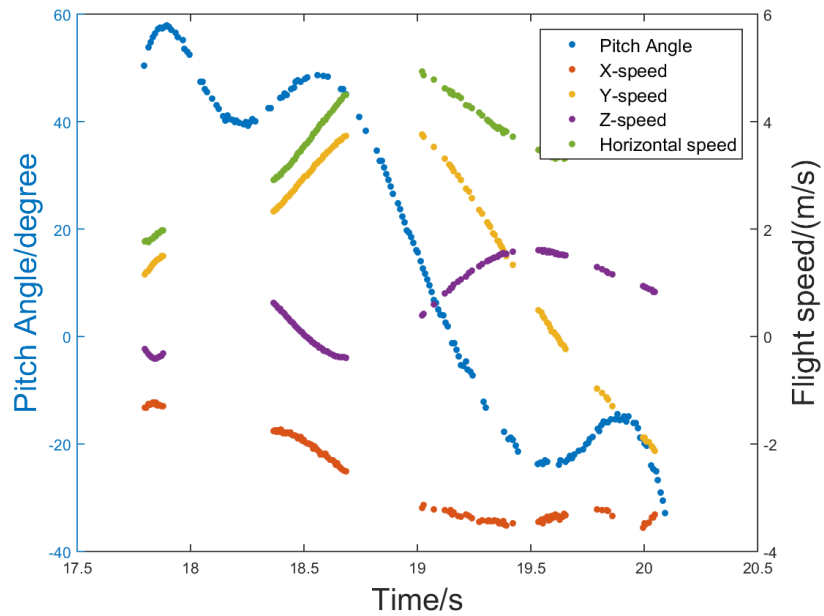


**Figure 4.4:** Pitch angle and flight speeds. The x axis represents time while the two y axes are pitch angle and flight speed, respectively. The blue color line represents the pitch angle and the other four lines represent speeds in different directions. From the plot, correlation between pitch and z direction speeds can be observed.

Correlation coefficients (Pearson's) between pitch angle and height or between pitch angle and speeds were calculated to quantitatively explore the correlations. Each pairs of quantities were calculated for correlation coefficients, and then the results were averaged for a more reliable representation. From Table 4.2, which recorded the correlation coefficients of different quantities with pitch angle. In the table, the height data was approximated using a polynomial of order 6, while the

speeds data were approximated by polynomials of order 10. From Table 4.2, all of the quantities have no obvious correlation with pitch angle expect for Z-Speed, which has a negative correlation of -0.596 and can be classified as correlated with pitch angle.

**Table 4.2:** Correlation coefficients between pitch angle and other specifications. The height data was approximated using polynomial of order 6 while the speeds data were approximated using polynomials of order 10. The correlation coefficients in the table are the average value from all trials of all beetles.

Compared Quantities	Height	X-Speed	Y-Speed	Z-Speed	H-Speed
Correlation Coefficients	0.0894	-0.037	0.020	-0.596	-0.059

After finding the possible correlation behind pitch angle and speeds. The correlation and coefficients between the vertical speed and pitch angle were calculated for different time differences. Figure 4.5 showed the average coefficients of one of the experimental beetles across different time-lags. The correlation coefficients are negative for all computed time-lags, which is coincided with the observation from Table 4.2. For this instance, a strong correlation is observed for coefficients that are larger than 0.6. And the largest absolute value occurs on the negative half of time axis, which is an indication of precedence of pitch angle over vertical speed in term of changing sequence.

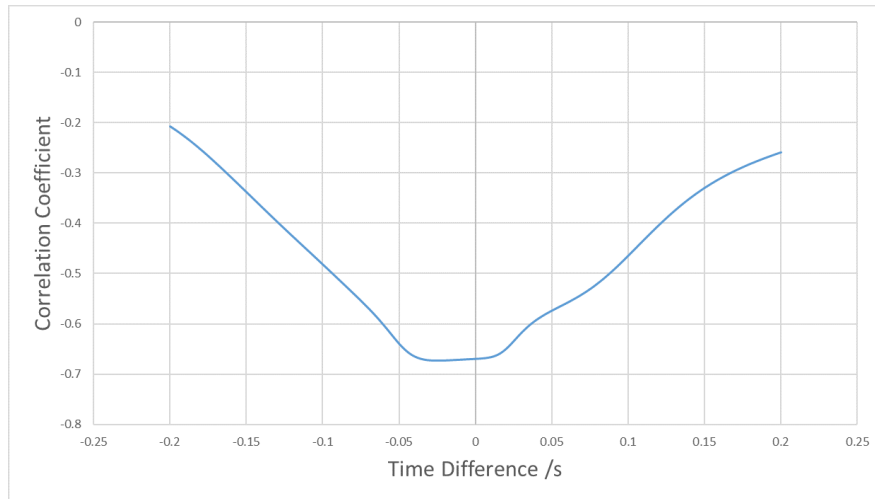


**Figure 4.5:** Correlation coefficients between pitch angle and z-speed with respect to time difference. The x axis is the time difference, representing the amount of time that z-speed curve being shifted in order to match with pitch angle. The maximum absolute coefficient occurs at negative time difference, which indicated that pitch angle changed before z-speed did.

And finally, the correlation between pitch angle and acceleration was also explored. Figure 4.6 shows how pitch angle and the three accelerations (along three

axis) changed with respect to time. Similarly, the blue line represents the pitch angle while the other three represent accelerations along x, y, and z directions. The x direction here refers to the direction along the longitudinal direction of beetle body but within the horizontal plane. And the y direction refers to the direction perpendicular to x direction within the same horizontal plane. Z direction is the upward vertical direction. From Figure 4.6, correlation between pitch angle and x-acceleration and z-acceleration seem to exist. Hence, further calculation of coefficients was required.

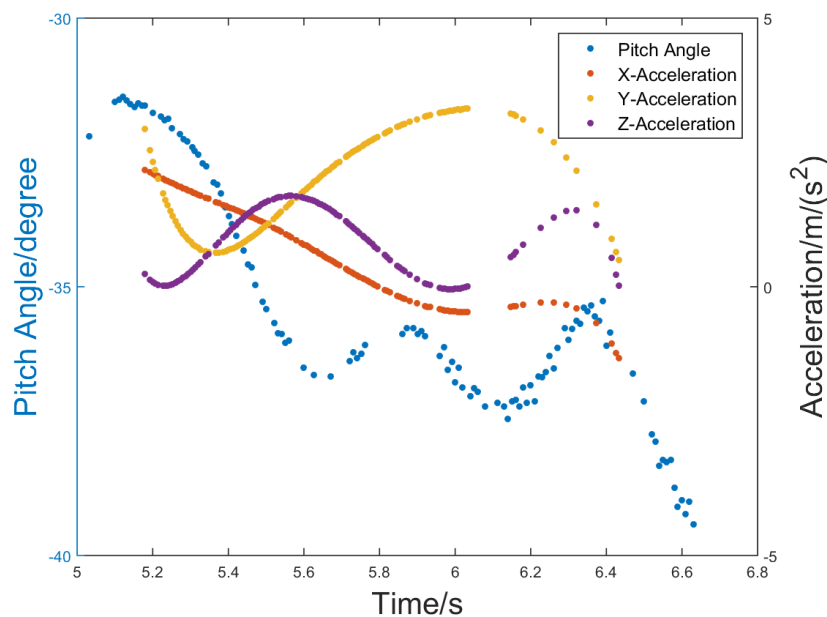


**Figure 4.6:** Pitch angle and flight accelerations. The x axis is time while the two y axes are pitch angle and accelerations, respectively. The blue color line represents the pitch angle and the other three lines represent accelerations in different directions. From the plot, correlation between pitch and x-acceleration and z-acceleration can be observed.

The calculated values of correlation coefficients were shown in Table 4.3. These coefficients were obtained by averaging many correlation coefficients of different combination of polynomial orders. And the polynomials order were tested from 4 to 12 for both pitch angle and accelerations. One example of these tests can be seen at Table 4.1. From the calculated result, strong correlation between pitch angle and x-acceleration was observed. However, there is poor correlation between pitch angle and the other two accelerations.

**Table 4.3:** Average correlation coefficients between pitch angle and accelerations. The average accelerations were obtained by averaging coefficients of different combinations of polynomial orders. The polynomial orders goes from 4 to 12 for both pitch angle and accelerations.

Accelerations	X-Acc	Y-Acc	Z-Acc
Average Coefficients	0.735	-0.220	-0.218

The correlation coefficients between pitch angle and x-acceleration was further explored by shifted the x-acceleration curve along the time axis in order to find a best match with pitch angle. Most parts of the line are above 0.5, which indicated a strong correlation. The maximum value occurs almost at zero time difference.

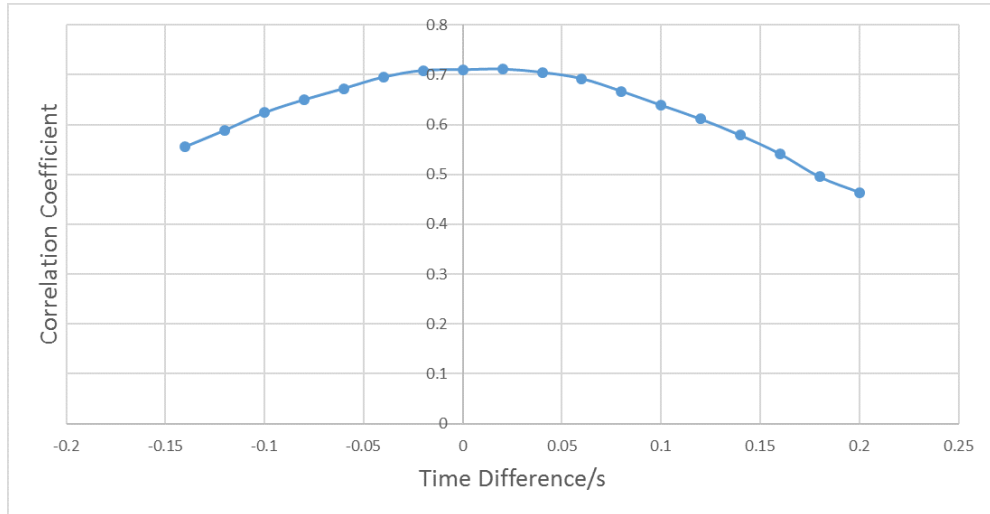


**Figure 4.7:** Correlation coefficients between pitch angle and x-acceleration across different time differences. The x axis represents the time differences in second, while the y axis represents the correlation coefficients. Most parts of the line are above 0.5, which indicated a strong correlation. The maximum value occurs almost at zero time difference.

## 4.5 The Effect of Pitch Angular Speed and Pitch Angular Acceleration

Using the original pitch angle data, pitch angular speed and angular acceleration were calculated. And then these new quantities were compared with the flight specifications again, similar to the previous sections. However, the calculation results, which are shown in Table 4.4, indicate that there is no obvious correlation between each pair.

**Table 4.4:** Correlation of specifications with pitch angular speed and pitch angular acceleration. The second row shows correlation coefficients between pitch angular speed and flight specifications, while the third row shows those between pitch angular acceleration and flight specifications.

Specifications	Coefficient 1	Coefficient 2
Height	0.1	0.072
X-Speed	0.173	0.074
Y-Speed	0.05	0.055
Z-Speed	0.345	0.261
H-Speed	-0.255	0.023
X-Acc	-0.026	-0.234
Y-Acc	-0.237	0.047
Z-Acc	-0.392	0.093

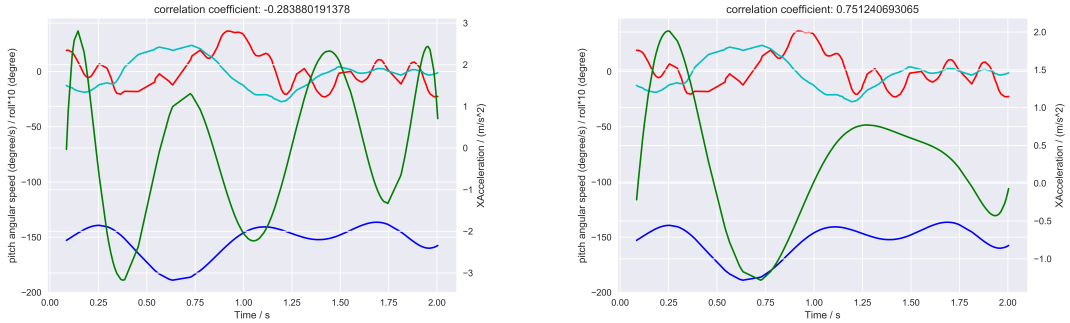
# Chapter 5

## Discussion

### 5.1 Discussion on Data Analysis

In Section 4.2, approximation using different orders of polynomials was illustrated. And in that section, a comparison of correlation coefficients of whether or not to approximate speeds data before calculating acceleration was done. The result showed that approximation has higher value of correlation coefficients. In Figure 5.1, the blue curves depict the pitch angle data after being approximated by an order 10 polynomial, while the green curves represent the x-acceleration after being approximated by an order 8 polynomial. The red and cyan curves are the change of roll angle and yaw angle, respectively. The two plot are generated from a same piece of original data. From Figure 5.1, the acceleration curve with a prior speeds approximation (on the right) has less cyclic fluctuations than that without a prior speeds approximation (on the left). The extra cyclic fluctuations might be caused by the cyclic drift of sensors, which is an error from the experimental apparatus. On the plots, there are correlation coefficients between the pitch angle and acceleration for the portion shown in the plots. As we can see, the left plot has a much lower (negative) coefficient than the right plot. The cyclic fluctuations greatly affect the result and it is considered as an unwanted noise for this reason since the overall shape of the curves was easily twisted by some extreme values in the original data.

After processing the data, further details between pitch angle and flight specifications were explored. The initial conjecture is that when beetle performs pitch down action, the speeds would increase, while the height might change differently since it depended on the state of the flight. For instance, if the beetle flies upwards when it is pitching down, the height will still be increased however the speed will



(a) No prior speeds approximation before calculating accelerations

(b) Prior speeds approximation before calculating accelerations

**Figure 5.1:** Comparison between curves without prior speeds approximation and that with speeds approximation. The blue curves depict the pitch angle data after being approximated by a order 10 polynomial, while the green curves represent the x-acceleration after being approximated by order 8 polynomial. The red and cyan curves are the change of roll angle and yaw angle, respectively. The only difference between the two graphs is the approximation of speed data before calculating accelerations. As shown on the left plot, which is the result of not having the approximation, the acceleration curve has more cyclic fluctuations than the plot on the right. The cyclic motions might be caused by the cyclic drift (error) of the sensors, which will greatly affect the result. And that is why the left plot has a much lower correlation coefficient than the right plot.

be reduced accordingly. The physical interaction between the wings of the beetle and the air is the essence underlying the changes of flight specifications. This consideration led to the investigation of the correlation between pitch angle and acceleration, which is the direct result from aerodynamic forces. When beetle performs pitch-down action, its stroke plane tilts forward [11], which resulted in an increase of forward acceleration (x axis along longitudinal direction of beetle body). Hence, it is proposed that the resulted x-acceleration had positive correlation with the pitch angle while the y-acceleration is supposed to have no obvious correlation. The z-direction is supposed to have negative correlation due to the direction setting of the body coordinate system.

The experimental result of pitch angle and height showed nearly no correlation for most of the trials, which meant when the beetle pitched downwards, the flight height increased or decreased with equal possibilities. The change of height is subjected to the vertical speed and the length of time. Different directions of current vertical speed (upwards or downwards) would result in different changes of flight height.

While the correlation between pitch angle and height is not obvious, the correlation between pitch angle and z speed is considerable. As initially proposed, the vertical speed should increase in negative direction when the beetle pitches downwards, which results in negative correlation coefficients. The maximum value occurs at the negative time axis, which means that pitch angle changed before the vertical speed changed, and that is coincided with the initial conjecture. The x speed and horizontal speed were supposed to be of strong correlation with pitch angle as well. However, the results show that there is no correlation between these quantities and pitch angle. This behavior may be caused by the different aerodynamics of flapping-wing mechanism. The y direction was in accord with the proposed behavior, which is the low correlation between them.

And finally, acceleration and pitch angle were paired for calculating correlation coefficients. The results show a strong correlation between pitch angle and x-acceleration for most segments. There are also a small amount of coefficients that are relatively small. The abnormality appeared cyclically in the data sets, which suggested that it might be due to the flight pattern of beetles. One of the possible reason is that flight behavior is affected by the environment, which is the size constraints of the experimental room that caused the beetles to perform avoidance flight pattern. During the avoidance pattern, namely a saccade, the beetles intensively and actively changed their wings' flapping pattern to generate aerodynamic forces allowing the body to have enough accelerations for turning. And during this period, the roll angle would also have effects on other flight specifications, resulting in the abnormal behavior. Another possibility will be due to the initial speed. Higher speed might had a different effect on flight acceleration change with pitch angle as compared with lower speed. And the direction of the initial speed may also result a different effect. The maximum coefficients between pitch angle and x-acceleration occurs almost at zero time difference, which indicates that the x-acceleration changes almost as soon as pitch angle does. The acceleration is a direct result from forces, and that is the reason why x-acceleration changes swiftly. Unlike the situation in exploring pitch angle and z-speed, since speed is an integration of acceleration over time, it requires longer time to change to a significant amount.

Apart from exploring the role of pitch angle, the role of pitch angular speed and pitch angular acceleration were also explored. Since in some past researches, there is evidence showing that pitching moment is an important factor of flight gesture

(Section 2.3). Here is the moment equation for pitch moment,

$$\begin{aligned}
 M &= F \times d = m \times a \times d \\
 &= m \times (\alpha \times d) \times d \\
 &= m \times d^2 \times \alpha \\
 &= I \times \alpha
 \end{aligned}$$

where  $I$  is the moment of inertia of beetle (consistence for one beetle), and  $\alpha$  is the pitch angular acceleration.

The equations lead to an exploration of the role of pitch angular acceleration in the flight. And since pitch angular speed is the intermediate product when calculating pitch angular acceleration, it was also taken into consideration.

However, the calculated results (Table 4.4) show no obvious correlation coefficient between the different pairs of quantities that were explored. The possible explanation here is that due to the huge size of the experimental beetles and the large inertia they possessed, the effect from pitching moment is not significant enough to change the whole body's flight specifications. It is different from the role of pitch angle, since the change of the pitch angle also represent a tilt of the stroke plane. And a tilt of stroke plane is the essential change of the wing dynamics, which subsequently changed the accelerations and speeds. Further exploration is needed to understand more about the physics and biology behind it.

## 5.2 Recommendations

Future study can focus on exploring and comparing the different roles of pitch angle, pitch angular speed and pitch angular acceleration. The project revealed the role of pitch angle in z-speed and x-accelerations. And more researches are required to be done to confirm these correlations and to find out the reasons behind those pairs with no clear correlations. Those pairs of quantities with nearly no correlation might be affected by some extreme cases which lower the averaged values. Possible reasons are the sudden change of wing-beating patterns and the initial flight speeds.

Correlation is not causation. Examination of causation takes years due to a large number of possibilities and the complicated underlying structure or principle. In order to correctly identify the cause of flight specifications, more researches and

experiments are needed to be done. The real biological essence of beetle's pitching control mechanism is still not clear due to the lack of biological development and limitation of current technologies. The controlling muscles have to be identified for further development of this topic. After the identification of beetle's control mechanism over pitching, stimulating experiments has to be performed to verify the effect of electrical stimulation and the practicability of control.

It is also necessary to investigate the pitching of beetle's wings during flight. The essential forces and moments behind a body pitching are mostly generated by the wings as wings are the only source of aerodynamic forces for beetles. To further support the development of this control method, aerodynamics analysis also has to be done in the future. Computational Fluid Dynamics Software (For example, ANSYS) can also be used to analyze the detailed force conditions during the flight, especially during the saccade.

The sensor data processing part can also be improved. Due to a huge amount of data collected, it is difficult for human to directly find out the underlying patterns of the data. A possible way to solve it is to apply machine learning method, like clustering, to classify data with common characteristics together. Machine learning algorithm can also be used for removing the noises or other unnatural behaviors of data.

# Chapter 6

## Conclusion

This report covers two major tasks of the final year project, which is a part of a huge research project, Beetle Flight Control. For the first part, programming on the circuit board that would be carried by the experimental beetles was required. The circuit board was programmed so that it can receive control signals from the remote computer terminal by radio frequency transmission. The signals were then interpreted to different specifications of electrical pulses, which are channel number, stimulating duration, pulse frequency, peak time duration, voltage value and initiation latency. Four channels of signal output were designed and programmed, which can work independently from each other. High impedance state was set for unused channels to prevent current flow in non-experimental muscles. Power management of the circuit board was also programmed to lengthen the battery life.

The second part of the project is exploring correlation between pitching and flight specifications: height, speeds and accelerations. Low correlation was observed between pitch angle and height, but higher correlation was observed for pitch angle and z direction speed. Finally, correlation between pitch angle and x direction acceleration appeared to be strong, but a small amount of weak correlation still existed. Reasons behind this inconsistent pattern might be the sudden change of flight pattern and different initial speeds before performing pitching action. Further analysis of wing-beating patterns using ANSYS is needed. The role of angular speed and angular acceleration were also explored, but the results showed no clear correlation in all the paired quantities.

The project served as an entomological research for beetle flight behavior, which will be greatly beneficial to the development of beetle flight control methods. Cor-

relation of pitch angle and flight specifications revealed the possibility of another path of controlling elevation and flight speeds, which is considered as less energy intensive as compared to methods of stimulating flight muscles using higher frequency of electric pulses and it may also interfere with other wings control signals. For example, the third-auxiliary muscles for controlling turning direction, may be interfered by the pitch angle adjusting signals. The control over pitch angle might be able to perform by stimulating the corresponding neural system. Further researches on the quantitative relation between the pitch angle and flight specifications, and even on the stimulus strength controlling pitching have to be done for freely controlling beetle in a three-dimensional space.

# Bibliography

- [1] Bozkurt A. et al. Balloon-assisted flight of radio-controlled insect biobots. *IEEE Transactions On Biomedical Engineering*, 56(9):2304–2307, 2009.
- [2] Bogue R. Recent developments in miniature flying robots. *Industrial Robot: An International Journal*, 37:17–22, 2010. doi: 10.1108/01439911011009920.
- [3] Sato H. et al. Deciphering the role of a coleopteran steering muscle via free flight stimulation. *Current Biology*, 25:798–803, 2015. URL <http://dx.doi.org/10.1016/j.cub.2015.01.0519>.
- [4] Michelsen A., Andersen B.B., Kirchner W.H., and Lindauer M. Honey bees can be recruited by a mechanical model of a dancing bee. *Naturwiss*, 76: 277–280, 1989.
- [5] Mecynorrhina torquata. URL [http://beetlespace.wz.cz/e\\_Mecynorrhina\\_torquata.html](http://beetlespace.wz.cz/e_Mecynorrhina_torquata.html).
- [6] Dudley R. *The Biomechanics of Insect Flight: Form, Function, Evolution*. Princeton University Press, 2000.
- [7] Sato H. et al. Remote radio control of insect flight. *Frontiers in Integrative Neuroscience*, 3(24), 2009. doi: 10.3389/neuro.07.024.2009.
- [8] Chung A.J., Cordovez B., Jasuja N., Lee D.J., Huang X.T., and Erickson D. Implantable microfluidic and electronic systems for insect flight manipulation. *Microfluid Nanofluid*, pages 345–352, 2012. doi: 10.1007/s10404-012-0957-z.
- [9] Maharbiz M.M. A cyborg beetle: Wireless neural flight control of a free-flying insect. *SBCCI '09 Proceedings of the 22nd Annual Symposium on Integrated Circuits and System Design: Chip on the Dunes*, (3), 2009. doi: 10.1145/1601896.1601900.

- [10] Elzinga M.J., Breugel F.V., and Dickinson M.H. Strategies for the stabilization of longitudinal forward flapping flight revealed using a dynamically-scaled robotic fly. *Bioinspiration and Biomimetics*, 9(2), 2014. doi: 10.1088/1748-3182/9/2/025001.
- [11] Sun M. Insect flight dynamics: Stability and control. *Reviews of Modern Physics*, 86, 2014. doi: 10.1103/RevModPhys.86.615.
- [12] Whitehead S.C., Beatus T., Canale L., and Cohen I. Pitch perfect: How fruit flies control their body pitch angle. *The Journal of Experimental Biology*, 218:3508–3519, 2015. doi: 10.1242/jeb.122622.
- [13] Taylor G.K. Mechanics and aerodynamics of insect flight control. *Biol Rev Camb Philos Soc*, 76(4):449–471, 2001.
- [14] Truong T.Q., Phan V.H., Sane S.P., and Park H.C. Pitching moment generation in an insect-mimicking flapping-wing system. *Journal of Bionic Engineering*, 11:36–51, 2014. doi: 10.1016/S1672-6529(14)60018-4.
- [15] Muijres F.T., Elzinga M.J., Iwasaki N.A., and Dickinson M.H. Body saccades of drosophila consist of stereotyped banked turns. *The Journal of Experimental Biology*, 218:864–875, 2015. doi: 10.1242/jeb.114280.